Measurement and Modeling of Solubility and Saturated-Liquid Density and Viscosity for Methane/Athabasca-Bitumen Mixtures

Hossein Nourozieh[1], **Mohammad Kariznovi**, and **Jalal Abedi**, University of Calgary

Summary

In the steam-based recovery processes, the coinjected gas can dissolve and diffuse into bitumen or heavy oil for viscosity reduction. The equilibrium concentration and solubility of methane are governed by the complex interaction with the bitumen. Thus, it is necessary to know the quantitative effects of gas dissolution on bitumen viscosity, density, and phase behavior at elevated temperatures in which steam-based processes are applied.

Thus, this study aims at providing necessary experimental data for methane/Athabasca bitumen over a wide range of temperatures and pressures (up to 190°C and 10 MPa); that is, conditions that approach the temperatures at in-situ steam processes. Our previously designed phase-behavior experimental apparatus was used to measure the solubility of methane in Athabasca bitumen and its corresponding saturated-phase properties. Then, the measured solubility and density data were modeled with the Peng-Robinson equation of state (EOS) (Robinson and Peng 1978).

The results indicate that the effect of temperature on the solubility profile of the methane/Athabasca-bitumen mixture is negligible at high temperatures and there is a distinct difference in the solubility data at 50°C compared with other isotherms (100, 150, and 190°C). Therefore, a reduction in viscosity at higher temperatures is much lower compared with a similar reduction at low temperature (50°C). There is a linear relationship between the methane-saturated viscosity and pressure for all temperatures in a semilog plot. The EOS modeling results also show that temperature-dependent binary-interaction parameters and volume-translation values should be considered to match density and solubility data.

Introduction

In-situ bitumen recovery from oil-sand formations in Canada has become economically feasible over the past 2 decades. Inventions and developments in recovery processes by use of steam-injection technology, such as steam-assisted gravity drainage (SAGD) and cyclic-steam stimulation, have contributed to this success (Butler and Stephens 1981; Butler 1985). Nonetheless, current steam-based processes are not optimal because they have very-high energy requirements for steam generation, making the processes economically vulnerable to high fuel prices. In addition, the quality of the product is poor (subject to a substantial differential in selling price) and so viscous that it requires dilution by expensive solvents to be transported by pipeline and accepted by heavy-oil refineries. Finally, substantial greenhouse gas emissions, large freshwater requirements for steam generation, the high cost of water treatments for reuse, and environmental concerns over wastewater disposal make current steam-based processes both economically vulnerable and environmentally damaging. Current recovery methods have been successful with water-based processes, but these processes are taxing to the environment and have been limited to higher-quality oil-sand deposits. Production from lower-grade deposits remains a technical challenge.

The disadvantages and economic concerns of the thermal processes make solvent-assisted processes such as vapor extraction (VAPEX) viable alternatives for the recovery of heavy oil and bitumen. In a solvent-injection process, the solvent injected into the reservoir is largely recoverable with the produced bitumen. Solvent also reduces the bitumen viscosity while using less energy, requiring less water, and avoiding carbon dioxide emissions. The main problem with the solvent-based processes is the low production rate.

To overcome the limitations of steam and solvent processes, the researchers proposed a hybrid process in which steam and solvent are coinjected. Numerous hybrid-processing schemes by use of both solvent and heat have recently been invented and patented. In these processes, the compound effects of solvent and heat on the bitumen viscosity could provide production rates equivalent to or higher than those attained by steam injection alone (Butler and Morkrys 1991; Gates 2007).

Experimental and modeling studies showed that, in steam-based processes such as SAGD, a small amount of methane as noncondensable gas can be coinjected with steam to improve the process performance. The process receives advantages from less steam consumption and less heat loss to overburden by providing thermal insulation (Butler et al. 2000; Al-Murayri et al. 2011). The injection of noncondensable gas in the SAGD process has been considered by many authors. Butler and Yee (1986) investigated the coinjection of methane and carbon dioxide with steam in a 1D sand-packed physical model. They proposed a mathematical model to predict the performance of the coinjection of noncondensable gas with steam, and their modeling results showed a beneficial effect.

Butler (1999) proposed a process called steam-and-gas push that improves the performance of the SAGD process. In this process, noncondensable gases are coinjected with steam. Physical-model experiments by Butler (1999) and Butler et al. (2000) confirmed the beneficial effect of the noncondensable-gas additive. The experiments showed that the noncondensable gas forms insulation at the edge of the chamber and reduces the heat loss. The effect of noncondensable-gas coinjection on the SAGD process has also been investigated by several authors (Edmunds et al. 1994; Goite et al. 2001; Bagci and Gumrah 2004; Al-Murayri et al. 2011).

When methane as a noncondensable gas is present in the steam chamber as a result of the coinjection process, it can dissolve and diffuse into bitumen or heavy oil. Diffusion and dispersion play important roles, whereas the understanding of the methane/bitumen interaction is vital for understanding the process. In a solvent-based process, such as VAPEX, methane can be coinjected with heavier solvents, such as propane and butane, to adjust the vapor pressure of solvent. Methane as a solution gas in the bitumen also affects the bitumen properties (density and viscosity) and controls the saturation pressure of initial reservoir oil.

The solvent-based recovery processes are currently hampered by limited data and modeling methodologies for solvent/heavy-oil and solvent/bitumen systems. This highlights that the phase behavior and thermodynamic properties of the mixtures containing heavy oil/bitumen and methane are extremely important for the coinjection processes. It is necessary to know how the methane additive affects oil properties at elevated temperatures before all the potential benefits can be determined. Indeed, the

[1]Now with Computer Modelling Group

Original SPE manuscript received for review 14 July 2014. Revised manuscript received for review 5 April 2015. Paper (SPE 174558) peer approved 14 April 2015.

SARA Fractions	
Saturates	12.26%
Aromatics	40.08%
Resins	36.53%
Asphaltenes	11.13%
Density at 23°C	1009 kg/m^3
Molecular weight	539.2±7.9 g/mol

Table 1—Properties of bitumen sample.

quantitative effects of methane on bitumen viscosity, density, and phase behavior are not well-understood, especially at elevated temperature in which the steam-based processes are applied. Thus, in this study, the available data for the phase behavior of methane/bitumen mixtures are reviewed and new data for methane/Athabasca bitumen are reported.

Background

The first attempt to measure the saturated properties of heavy oil and bitumen diluted with methane was implemented in 1980, with Jacobs et al. (1980) measuring the viscosity of methane-saturated Athabasca bitumen. The authors measured the viscosity of methane-saturated Athabasca bitumen in the temperature range of 23–120°C and at pressures up to 13.8 MPa. Svrcek and Mehrotra (1982) also measured the solubility and saturated-phase density and viscosity for methane/Athabasca-bitumen mixtures at temperatures up to 100°C and at pressures up to 10 MPa.

Mehrotra and Svrcek (1985a) reported the experimental data on the solubility and saturated-phase density and viscosity for methane/Peace-River-bitumen mixtures at temperatures up to 115°C and at pressures up to 10 MPa. In a subsequent study, Mehrotra and Svrcek (1985b) obtained the same measurements for methane/Wabasca-bitumen mixtures.

Fu et al. (1988) presented the vapor/liquid equilibrium properties of methane/Cold-Lake-bitumen mixtures by use of a modified Ruska rocking-cell apparatus for temperatures and pressures up to 150°C and 12 MPa, respectively. The authors only reported the composition of each phase at equilibrium condition during the phase-behavior studies. Mehrotra and Svrcek (1988) also reported the solubility data and the saturated-phase density and viscosity for methane/Cold-Lake-bitumen mixtures in the temperature range of 15–103°C and pressures up to 10 MPa. Frauenfeld et al. (2002) measured the solubility of methane in Lloydminster Aberfeldy oil at temperature of 19°C and at pressures up to 5 MPa. In a previous study by Zirrahi et al. (2014), the authors modeled the solubility of methane, ethane, nitrogen, carbon monoxide, and carbon dioxide in bitumen by use of available literature data, which were at temperatures lower than 100°C. No modeling study for saturated-liquid density and viscosity and no new data were presented by Zirrahi et al. (2014).

There are limited phase-behavior data of bitumen/methane mixtures in the literature for temperatures higher than 100°C. Although some experimental data for the methane/Cold-Lake-bitumen mixture at 150°C were reported by Fu et al. (1988), there is a lack of experimental data for density and viscosity of saturated-liquid phase. This study aims to provide necessary experimental data for methane/Athabasca bitumen over a wide range of temperatures and pressures; that is, the conditions approach the temperatures in the in-situ steam processes. The data provide necessary information for the properties of Athabasca bitumen when the methane exists as solution gas in bitumen and/or is dissolved in the bitumen. Thus, the designed experimental apparatus in our previous study (Nourozieh et al. 2012) was used to measure the solubility of methane in Athabasca bitumen and its corresponding saturated-phase properties. Then, the measured solubility and density data were modeled with the Peng-Robinson equation of state (Robinson and Peng 1978).

% Off	Temperature (°C)
Initial boiling point	192.4
5	277.6
10	320.1
15	353.8
20	385.1
25	415.0
30	441.9
35	470.3
40	500.4
45	531.2
50	564.7
55	596.3
60	623.7
65	645.9
70	665.9
75	689.5
80	713.3

Table 2—Compositional analysis of bitumen sample.

Experiment

Materials. The methane was supplied by Praxair with a purity of 99.97 mol%. The bitumen sample was provided by an oil company, which was operating a steam-assisted-gravity-drainage (SAGD) project (Surmont project) in southeast Fort McMurray, Alberta, Canada. The bitumen sample was taken from the production unit, and the sample was processed to remove sand and water. The water was removed from the bitumen by distillation, and the sand was removed by centrifuge. The density of the bitumen sample was measured with an Anton Paar density-measuring cell and was 1009 kg/m^3 at 23°C and atmospheric pressure. The molecular weight of the bitumen sample was measured by use of the cryoscopy method, which is dependent on freezing-point depression. Benzene was used as solvent, and the solutions were prepared to have 0.15 molal concentrations. This value is within the range recommended by the factory (Cryette) for the molecular-weight measurements. The average molecular-weight bitumen on the basis of four different measurements is 539.2±7.9 g/mol. The saturates/aromatics/resins/asphaltenes (SARA) analysis—a modified version of the American Society for Testing and Materials (ASTM) D2007 (2011) clay/gel-adsorption chromatography method—was conducted on the sample to separate different fractions by use of an *n*-paraffin solvent and the adsorption of fractions on clay or silica gel. The asphaltene fraction of bitumen is precipitated with *n*-heptane. The resin fraction is adsorbed on attapulgus clay, whereas the aromatic fraction is adsorbed on silica gel. The SARA compositional analysis of bitumen is presented in **Table 1.**

The bitumen sample was also subjected to compositional analyses to obtain carbon-number distributions up to C_{100} by use of the standard test method, ASTM D7169-11 (2011). This test method was used to determine the boiling-point distribution through a temperature of 720°C, which corresponds to the elution of *n*-C_{100}. The boiling-point distribution for the bitumen sample is given in **Table 2.**

Apparatus. The details of the experimental apparatus and its validation were presented previously (Kariznovi et al. 2011; Nourozieh et al. 2012). It consists of feeding cells, an equilibration cell, four sampling cells, a density-measuring cell, a viscometer, and two Quizix automated pressure-activated pumps. The Quizix

pumps charge and discharge water to displace the fluids or maintain constant pressure. The equilibration, sampling, and feeding cells are equipped with pistons to prevent the contamination of the mixture with water. The pistons are sealed with Viton O-rings supported by Teflon backup rings.

The equilibration and sampling cells, density-measuring cell, and viscometer are placed in a temperature-controlled Blue M oven. Two Quizix pumps control the pressure of the system. The rocking action of the equilibration cell with the rolling ball expedites the mixing process and reduces the time required to reach the equilibrium condition. The density-measuring cell and viscometer are used for phase detection and accurate volume measurements.

The Anton Paar custom densitometer has been used to measure fluid density. The densitometer was calibrated with nitrogen and water by use of the wide-range calibration method. The Cambridge viscometer was used to measure viscosity in the range of 0.2–10,000 cp. The viscometer is equipped with a sensor (SPL-440), which is factory calibrated. The pressure inside the apparatus was measured and controlled by different pressure transducers. An inline pressure transducer was installed, and the transducer is a Rosemount 3051CG5A capable of measuring pressure from –0.1 to 13.8 MPa (–14.2 to 2,000 psig), with an accuracy of 0.04%. The Quizix pumps were also equipped with pressure transducers. A Blue M oven was used to maintain the temperature during the experiments. The oven was equipped with a temperature controller capable of maintaining the temperature within ± 0.1°C. The temperature range of the oven was 15°C higher than ambient to 350°C.

Procedure

Before each experiment, the entire system was thoroughly cleaned to remove any potential contaminants including oil and solid particles. Toluene, acetone, and similar solvents were used to clean and remove bitumen, water, and any contaminants from the cells. To ensure that contaminants were not left inside the system, the cells and lines were successively evacuated and flushed with dry helium.

Bitumen was charged into the equilibration cell by use of two Quizix pumps. The mass of the bitumen inside the equilibration cell was obtained by measuring its volume and density at a constant temperature and pressure. Next, the solvent was charged into the cell following the same procedure. In this way, the mass fraction of the injected fluids was calculated.

The equilibration cell was rocked to improve mixing for the solvent/bitumen system at fixed temperature and pressure. During the mixing period, the volume of water that was charged or discharged to maintain a constant pressure in the equilibration cell was recorded. Equilibrium was achieved when no change in the cumulative volume of the water was observed. To discharge the saturated bitumen from the top of the rocking cell, the equilibration cell was kept in a vertical position for a few hours so that the single bulk volume of each phase becomes vertically segregated in the order of phase density. Following this, the equilibrium fluids were discharged through the density-measuring cell and viscometer, maintaining a constant temperature and pressure. Both the in-line and Quizix-pump pressure transducers measured the pressure. The value reported by the in-line pressure transducer, which was the exact system pressure, was reported as the equilibrium pressure.

The phase samples were collected with steady readings of the viscometer and the density-measuring cell, where any change in density and viscosity indicated the passage of a phase boundary through the measuring instruments. Liquid(s) and vapor phases were transferred into sampling cells 1 through 3, and the last sampling cell was used to purge the phase-boundary portion and clean the transition between the phases. The heavier phases completely displaced the lighter phases, which were vertically segregated in the order of phase density. This resulted in clean samples with sharp density variation. The volume of each phase was measured by monitoring the volume of water charged into the equilibration cell. Saturated samples were collected through the sampling port for compositional analysis and further study.

To measure the composition of the gas-saturated liquid(s), the collected samples were flashed into atmospheric pressure. The Chandler Engineering gasometer (Model 2331) was used to measure the volume of the evolved gas. The gasometer measured the volume of the gas with 0.2% accuracy and reported the corresponding gas temperature. The liquid sample was heated to ensure that all the dissolved gas was evolved from the oil. The solubility was calculated by use of the volume of evolved gas reported by the gasometer and the density of the gas at atmospheric condition.

Equilibrium Verification

As previously mentioned, the total volume of the equilibrium cell was monitored during the mixing at fixed pressure and temperature for phase-behavior studies presented here. At constant pressure, no change in the equilibrium-cell volume indicated that the mixture is fully saturated with methane and no more methane could be dissolved in bitumen. Thus, during the equilibration, the total volume of the equilibrium cell (vapor and liquid) was being recorded and monitored to control the mixing and determine the time when equilibrium was established. To ensure that the equilibrium condition was the real state of the system, some experiments at different temperatures were repeated, and the experimental results were compared. The measurements of saturated-phase densities are precise to less than 1.0 kg/m^3, and the deviations for saturated-liquid viscosities and solubilities are less than 5 and 6%, respectively.

Results and Discussion

In total, 20 combinations of temperatures and pressures (four temperatures of 50, 100, 150, and 190°C; five pressures of 1, 2, 4, 6, and 8 MPa) were considered for the measurements. The experimental data of solubility, saturated-phase density, and saturated-phase viscosity were reported for each experiment. For all experiments, a clear phase transition between two phases, vapor and liquid, was observed. **Fig. 1** illustrates phase transitions at four temperatures (50, 100, 150, and 190°C) and at selected pressures. As depicted in Fig. 1, both phases were completely segregated and a uniform phase in terms of density was detected during sampling. The vapor-phase densities were close to those of pure methane (within ± 0.5 kg/m^3 for all experiments at different temperatures), which shows that the vapor phase at equilibrium condition was virtually pure methane.

The experimental results for solubility and saturated-phase density and viscosity for methane/Athabasca-bitumen mixtures are summarized in **Table 3.** As Table 3 shows, the dissolution of methane in bitumen results in the change in the liquid density and viscosity. The solubility of methane in bitumen is a function of temperature and pressure; that is, the solubility increases with pressure at a constant temperature, which results in a reduction in the density and viscosity of liquid phase. Although the variation in temperature does not significantly change the solubility of methane, the increase in temperature lowers the solubility. Note that the variation of methane-saturated liquid viscosity with pressure is more considerable at temperature of 50°C (lowest temperature) compared with other temperatures. This can be explained in two ways: The bitumen viscosity is more pressure-dependent at lower temperatures, and at lower temperatures, the solubility is higher and the effect of pressure on the solubility and viscosity is higher.

Fig. 2 illustrates the solubility of methane in Athabasca bitumen as function of pressure at different temperatures. The solubility generally increases with the pressure at fixed temperature for all temperatures and decreases with the temperature for all pressures. The results indicated that the solubility of methane in Athabasca bitumen is less than 1.5 wt% of methane in the studied temperature and pressure ranges.

As anticipated from Fig. 2, the difference between isothermal-solubility lines is higher at lower temperature, but this difference diminishes rapidly with temperature. For instance, at high temperatures (e.g., 150 and 190°C), there is no significant difference (average of <0.03 wt%) between the two isotherms. This indicates that the effect of temperature on the solubility of methane at high temperature is not considerable. Nevertheless, at the lowest temperature, 50°C, the solubility of methane shows a distinct difference compared with the other isotherms. Pressure induces a larger

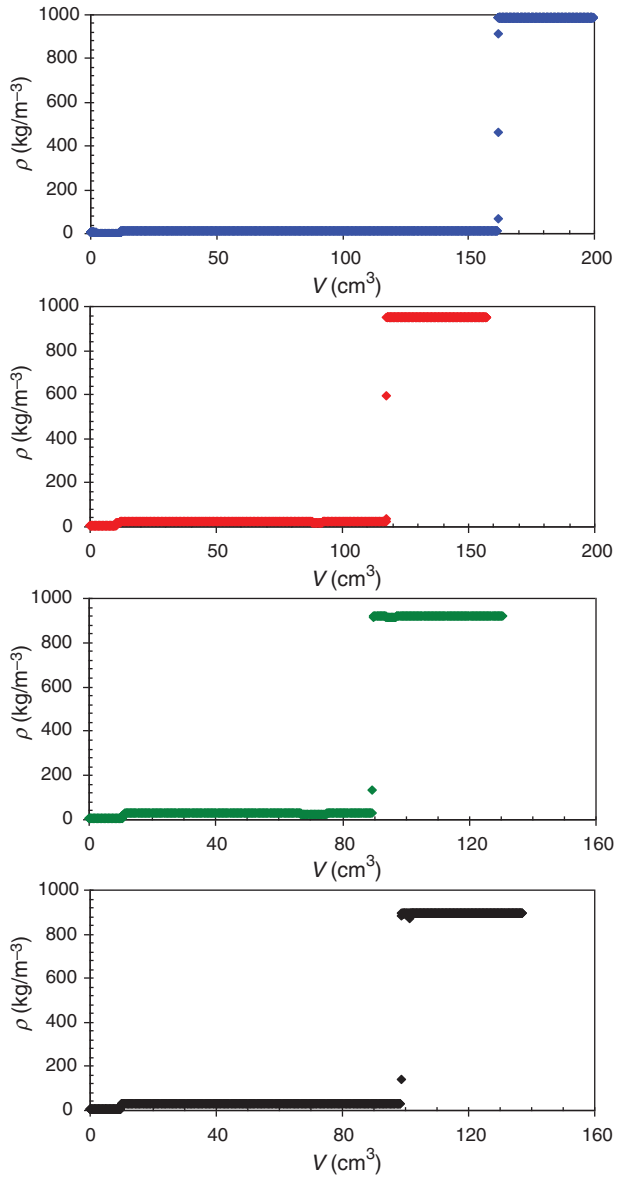

Fig. 1—Phase transitions for vapor/liquid-equilibrium study of methane/bitumen mixtures: blue, 50°C and 2 MPa; red, 100°C and 4 MPa; green, 150°C and 6 MPa; black, 190°C and 8 MPa.

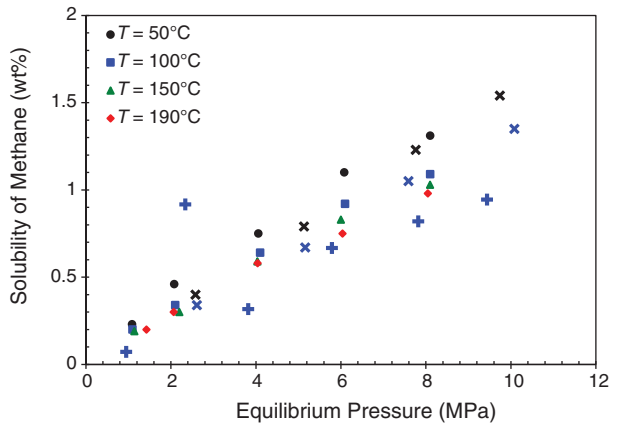

Fig. 2—Measured solubility of methane in Athabasca bitumen as a function of pressure at different temperatures: × symbols are Mehrotra and Svrcek (1988), and + symbols are Svrcek and Mehrotra (1982).

T (°C)	P (MPa)	W_s (fraction)	ρ_s (kg/m^3)	μ_s (mPa·s)
50.1	1.089	0.23	991	11900
49.9	2.082	0.46	989	8570
50.1	4.061	0.75	984	5230
51.4	6.081	1.10	979	3460
52.4	8.100	1.31	975	2340
100.2	1.100	0.20	958	201
100.3	2.103	0.34	956	183
100.2	4.102	0.64	952	148
100.3	6.101	0.92	948	125
100.2	8.100	1.09	944	115
149.8	1.142	0.19	928	31.4
149.9	2.201	0.30	925	29.1
150.1	4.033	0.59	922	25.6
150.3	5.998	0.83	918	24.3
149.9	8.097	1.03	914	21.6
189.8	1.427	0.20	905	11.7
189.8	2.068	0.30	904	11.4
190.2	4.040	0.58	901	10.7
189.5	6.039	0.75	897	9.8
189.3	8.045	0.98	893	9.2

Table 3—Experimental vapor/liquid-equilibrium properties for methane/Athabasca-bitumen mixtures at T, temperature; P, pressure; ρ_s, saturated-liquid density; μ_s, saturated-liquid viscosity; and w_s, weight fraction of methane in saturated-liquid phase.

change in the methane solubility than temperature. An increase in pressure from 1 to 8 MPa increases the solubility from almost 0.2 to 1 and 1.3 wt% at temperatures of 190 and 50°C, respectively. However, the maximum solubility changes at pressure of 8 MPa, for which the solubility increased from 0.98 to 1.3 wt%.

The data by Mehrotra and Svrcek (1988) at temperatures of 46 and 103°C and Svrcek and Mehrotra (1982) at 100°C are also shown in Fig. 2. Although the solubility data of this study demonstrate slightly higher values compared with those studies, the measurements are close and the trends are the same. The observed deviation is mainly because of bitumen-sample preparation and variation in the properties of provided samples.

Figs. 3 and 4 demonstrate the viscosity and density, respectively, of methane-saturated Athabasca bitumen as a function of equilibrium pressure. The gas-free bitumen viscosity and density at each temperature are also shown in the plots on the y-axis. For all temperatures, a linear relationship between the methane-saturated viscosity and pressure exists in a semilog plot. However, at temperature of 50°C, the saturated-phase viscosity shows a nonlinear behavior.

At high temperatures (e.g., 190°C), viscosity reduction is less than at low temperatures (e.g., 50°C), and similar to the solubility trend, the isotherms are closer at high temperatures. The variation in saturated-phase viscosity at the highest temperature is negligible. This may be because of low solubility of methane in bitumen at high temperatures, which results in a slight change in viscosity with pressure. In addition, at high temperature, the bitumen viscosity is already reduced by temperature and the dissolution of a small amount of methane does not make considerable changes in viscosity. In contrast to solubility, temperature induces a larger change to the methane-saturated viscosity than pressure. This is because of the pronounced effect of temperature on pure-bitumen viscosity.

Although the methane solubilities show negligible changes with temperature at a constant pressure, the variation of the

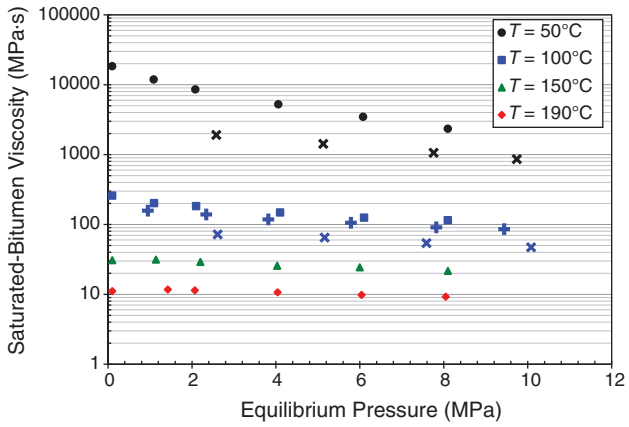

Fig. 3—Viscosity of methane-saturated Athabasca bitumen as a function of pressures at different temperatures: × symbols are Mehrotra and Svrcek (1988), and + symbols are Svrcek and Mehrotra (1982).

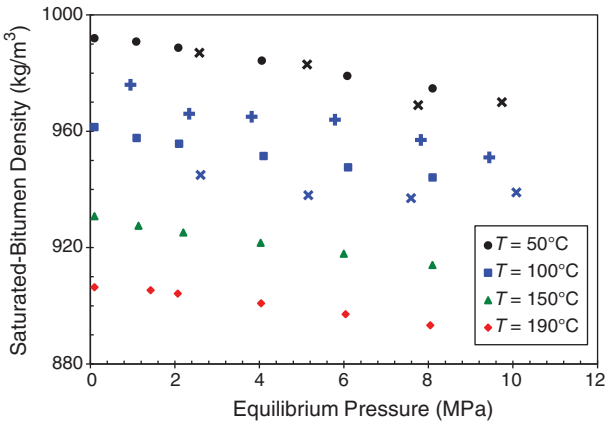

Fig. 4—Density of methane-saturated Athabasca bitumen as a function of pressure at different temperatures: × symbols are Mehrotra and Svrcek (1988) and + symbols are Svrcek and Mehrotra (1982).

saturated-bitumen densities with respect to pressure is not identical. The slope of variations reduces with the temperature, showing that a slight increase in the solubility results in a significant change in the density. For example, the slope of decreasing trend in the saturated-bitumen densities is increased approximately 30% when the temperature reduces from 190 to 50°C. It can be explained by the fact that the density is highly sensitive to the solubility of methane, and even a negligible increase in solubility can result in a considerable change in saturated-liquid density.

The gas-saturated density and viscosity data by Mehrotra and Svrcek (1988) at temperatures of 46 and 103°C and Svrcek and Mehrotra (1982) at 100°C are also shown in Figs. 3 and 4. Mehrotra and Svrcek (1988) used a bitumen sample that was originally lighter than the sample used in this study. Thus, the gas-saturated densities and viscosities at an isotherm are slightly lower in their studies compared with this study.

Modeling. The simulated-distillation data for the bitumen sample was used for bitumen characterization. Therefore, on the basis of the distillation data, 94 hydrocarbon components were assigned to the distillable fraction of bitumen. The characterization is based on the carbon-number group, from C_7 through C_{100} (Nourozieh et al. 2015). The boiling point of each component is related to carbon number through the equation developed by Riazi (2005):

$$T_b = 1090 - \exp(6.9955 - 0.11193N_c^{2/3}), \quad \ldots\ldots\ldots\ldots (1)$$

where T_b is the boiling point in K. Riazi (2005) developed two correlations for calculating the molecular weight (MW) and specific gravity (SG) of the carbon-number group up to C_{100}. The MW of each pseudocomponent was calculated by Eq. 2 developed by Riazi (2005) by use of the boiling point calculated by Eq. 1. Then, the SG is obtained from the calculated MW by use of Eq. 3. Thus, the MW and SG of each component are obtained by:

$$MW = \left[\frac{6.97996 - \ln(1080 - T_b)}{0.01964}\right]^{3/2}, \quad \ldots\ldots\ldots\ldots (2)$$

$$SG = 1.07 - \exp\left(3.56073 - 2.93886MW^{0.1}\right). \quad \ldots\ldots\ldots (3)$$

These 94 pseudocomponents represent the distillable fraction of bitumen, and the boiling points of defined components along with their compositions should accurately represent the distillation curve of bitumen samples. However, the asphaltene fraction of bitumen remained uncharacterized. In this study, the asphaltene is considered as one pseudocomponent. An average MW of 2000 g/mol was assigned to the heavy fraction (asphaltene fraction) of bitumen on the basis of the study by Diaz et al. (2011). The SG of this fraction was obtained from the correlation developed by Alboudwarej et al. (2003):

$$SG = 0.670MW^{0.0629}. \quad \ldots\ldots\ldots\ldots\ldots\ldots\ldots (4)$$

On the basis of this characterization scheme, the 94 pseudocomponents—single-carbon-number (SCN) fraction—were defined for the distillable fraction of bitumen, and one pseudocomponent was considered for the undistillable (asphaltene) fraction. The boiling point, MW, and SG of the SCN for the distillable fraction were calculated by Eqs. 1 through 3.

The other pseudocomponent properties, such as critical properties and acentric factor, are obtained by use of available correlations by use of the SG and boiling point. Svrcek and Mehrotra (1982, 1989) and Mehrotra et al. (1985) examined a number of these correlations for predicting the critical properties of Alberta bitumen and found that the Kesler and Lee (1976) correlations were the most appropriate for bitumen/gas systems. Modeling studies by Kariznovi et al. (2010) and Diaz et al. (2011) also indicated that the Kesler and Lee (1976) correlation provides better fit of the phase boundaries. They have tested different correlations to find which one can make acceptable predictions when they are applied to nondistillable fractions. Thus, in this study, the critical properties and acentric factor were obtained from the correlation proposed by Kesler and Lee (1976). The critical volumes of the components were calculated from the Twu (1984) correlation.

The pseudocomponent and critical properties are required properties for equation-of-state (EOS) modeling. For this study, the modified Peng-Robinson (Robinson and Peng 1978) EOS was used to calculate the saturation pressure for the primary characterization of bitumen:

$$P = \frac{RT}{v-b} - \frac{a\lambda(T)}{v(v+b)+b(v-b)}, \quad \ldots\ldots\ldots\ldots\ldots (5)$$

where

$$a = \frac{0.45724R^2T_c^2}{P_c}, \quad \ldots\ldots\ldots\ldots\ldots\ldots\ldots (6)$$

$$b = \frac{0.07780RT_c}{P_c}, \quad \ldots\ldots\ldots\ldots\ldots\ldots\ldots (7)$$

$$\lambda(T) = [1 + \kappa(1 - T_r^{1/2})]^2, \quad \ldots\ldots\ldots\ldots\ldots\ldots (8)$$

$$\kappa = 0.37464 + 1.5422\omega - 0.26992\omega^2, \quad \omega < 0.5, \ldots\ldots (9a)$$

$$\kappa = 0.379642 + 1.48503\omega - 0.164423\omega^2 + 0.016666\omega^3, \quad \omega \geq 0.5. \quad \ldots\ldots\ldots\ldots\ldots (9b)$$

The van der Waals mixing rules were used in this work to obtain the EOS parameters for the multicomponent mixtures:

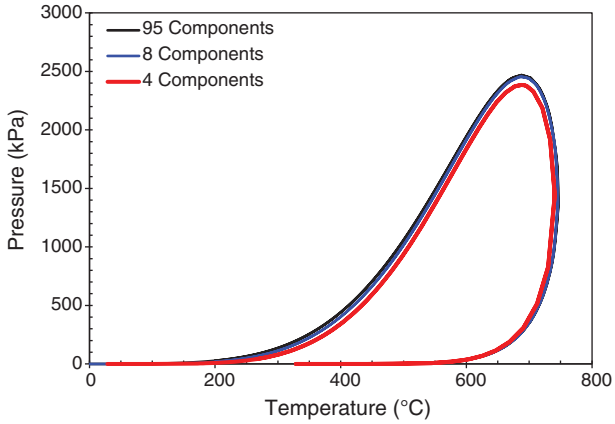

Fig. 5—Pressure/temperature diagram for different sets of pseudocomponents.

$$a_m = \sum_i x_i D_i, \quad \ldots\ldots\ldots\ldots\ldots\ldots\ldots\ldots\ldots\ldots (10)$$

$$b_m = \sum_i x_i b_i, \quad \ldots\ldots\ldots\ldots\ldots\ldots\ldots\ldots\ldots\ldots (11)$$

with

$$D_i = \sqrt{a_i}\sum_j x_j(1-\delta_{ij})\sqrt{a_j}, \quad \ldots\ldots\ldots\ldots\ldots\ldots (12)$$

where δ_{ij} is the interaction coefficient for the binary pairs within the mixture. The interaction coefficients are adjusted to fit the experimental equilibrium data. The binary-interaction parameters can be considered as constant values or defined on the basis of the critical properties. These parameters can be related to critical volume of components through the following equation (Oellrich et al. 1981):

$$\delta_{ij} = 1 - \left(\frac{2v_{ci}^{1/6}v_{cj}^{1/6}}{v_{ci}^{1/3}+v_{cj}^{1/3}}\right)^n. \quad \ldots\ldots\ldots\ldots\ldots\ldots (13)$$

Oellrich et al. (1981) showed that a value of 1.2 for n provided a good match for paraffin/paraffin-interaction coefficients. However, in this study, n was considered as a matching parameter to fit the equilibrium data.

After bitumen characterization, it is required to lump or group the pseudocomponents into fewer numbers of pseudocomponents. Lumping may reduce the accuracy of predictions, but it will save run time. Depending on the system under study, the number of appropriate pseudocomponents may differ; for instance, in systems near the critical point, by changing the number of pseudocomponents, the system behavior and stability may change. In addition, the procedure of choosing these groups from original fluids and the calculation of pseudocomponent properties are the main issues (Whitson 1983).

The pressure/temperature two-phase envelope was obtained with the Peng-Robinson EOS (Robinson and Peng 1978) by use of the full number of components; 95 defined pseudocomponents were then lumped into a number of pseudocomponents as the pressure/temperature diagram was generated and compared with the full-characterization scheme. The Lee and Kesler (1975) mixing rule was used to calculate the critical properties of lumped components. **Fig. 5** illustrates the generated pressure/temperature diagram for Athabasca bitumen by use of the full number of components and eight and four pseudocomponents. As depicted in Fig. 5, Athabasca bitumen can be represented by four pseudocomponents. The properties of the lumped pseudocomponents are summarized in **Table 4.**

As previously discussed, the interaction parameters between different pseudocomponents were considered as tuning parameters to match the solubility data or saturation pressures. Considering two different exponents (Eq. 13)—one for the pseudocomponent/pseudocomponent interaction, one for the methane/pseudocomponent interaction—did not improve the predictions. Thus, one exponent representing all interactions was adjusted and it was found that a value of –0.737 for n gave the lowest average absolute relative deviation (AARD) (14%) by use of four pseudocomponents. **Fig. 6** compares the predicted solubilities by use of four pseudocomponents against the experimental data. As depicted in Fig. 6, the solubilities are reasonably predicted with the EOS over a wide range of pressures and temperatures.

Although considering the temperature-dependent binary-interaction parameters could improve the model predictions, a single exponent also represents the solubility data well. The calculated AARD by use of temperature-dependant binary-interaction parameters was 9.9%. This value was obtained by adjusting the exponent of the binary-interaction parameters for each temperature **(Table 5).**

Prediction of Liquid Densities

Equation of State (EOS). The volumetric properties of bitumen and gas-saturated bitumen can also be calculated by EOS. Peneloux et al. (1982) proposed a volume-translation technique to improve the volumetric results for the Peng-Robinson EOS (Robinson and Peng 1978). In the Peneloux et al. (1982) technique, a certain translation along the volume axis can be applied, whereas the other equilibrium properties remain unchanged. Therefore, the density predictions were improved, while the other properties would not be affected. The corrected volume is obtained by

$$v^{\text{cor}} = v - c, \quad \ldots\ldots\ldots\ldots\ldots\ldots\ldots\ldots\ldots\ldots (14)$$

where v^{cor} is the corrected molar volume and c is a matching parameter, which is obtained from experimental data. For multicomponent systems, the c can be obtained by

$$c = \sum_{i=1}^{N} x_i c_i, \quad \ldots\ldots\ldots\ldots\ldots\ldots\ldots\ldots\ldots\ldots (15)$$

where x_i is the mole fraction of component i in the mixture.

$$c_i = \Omega_b v_s^i \frac{RT_c}{P_c}, \quad \ldots\ldots\ldots\ldots\ldots\ldots\ldots\ldots\ldots\ldots (16)$$

where P_c is the critical pressure, T_c is the critical temperature, Ω_b is EOS constant (for the Peng-Robinson EOS (Robinson and Peng 1978), it is 0.077796), and v_s is the volume translation that can be a tuning parameter and is obtained by matching experimental data.

Thus, the volume translation was applied to the lumped components to match the bitumen and saturated-liquid densities.

By use of temperature-independent volume-shift values, the saturated-liquid densities were inaccurately modeled with the

Component	MW (g/mol)	T_c (°C)	P_c (MPa)	ω	SG
PC1	209.9	450.2	2.34	0.547	0.888
PC2	379.0	587.7	1.50	0.869	0.955
PC3	886.5	756.3	0.81	1.308	1.027
PC4	2140.0	961.1	0.55	1.584	1.156

Table 4—Properties of pseudocomponents for Peng-Robinson EOS (Robinson and Peng 1978). MW, molecular weight; T_c, critical temperature; P_c, critical pressure; ω, acentric factor; and SG, specific gravity.

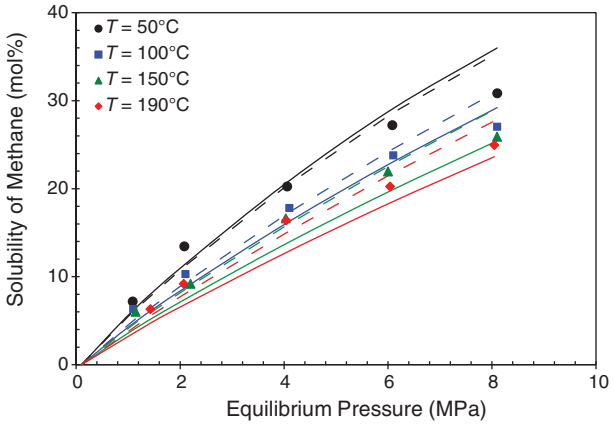

Fig. 6—Comparison of measured (symbols) and predicted solubilities of methane in Athabasca bitumen as a function of equilibrium pressure at different temperatures: solid line, temperature-independent binary-interaction coefficients; dashed line, temperature-dependent binary-interaction coefficients.

EOS. Thus, it is required to define temperature-dependent volume-shift values. The volume shift was represented by the following relation (Pedersen et al. 2004):

$$v_s^i = v_{s0}^i + v_{s1}^i (T - T_{\text{ref}}). \quad \ldots\ldots\ldots\ldots\ldots\ldots\ldots\ldots (17)$$

Component-volume shifts were calculated by Rackett's *Z*-factor correlation (Kokal and Sayegh 1990):

$$v_s = \left(\frac{RT_c}{P_c}\right) Z_{RA}^{[1+(1-T_r)^{2/7}]}. \quad \ldots\ldots\ldots\ldots\ldots\ldots\ldots\ldots (18)$$

Fig. 7 presents the calculated gas-saturated-liquid densities along with the experimental values. As depicted in Fig. 7, the saturated-liquid densities are well-represented with the temperature-dependent volume-translation technique.

Effective Liquid Densities. The density of the mixtures with a dissolved gas can be predicted by

$$\rho_m = \frac{1}{\dfrac{w_s}{\rho_s} + \dfrac{1 - w_s}{\rho_B}}, \quad \ldots\ldots\ldots\ldots\ldots\ldots\ldots\ldots (19)$$

where w_s is the weight fraction of dissolved gas and ρ_s and ρ_B are the effective liquid density of gas and the density of bitumen, respectively. Tharanivasan et al. (2011) proposed a method

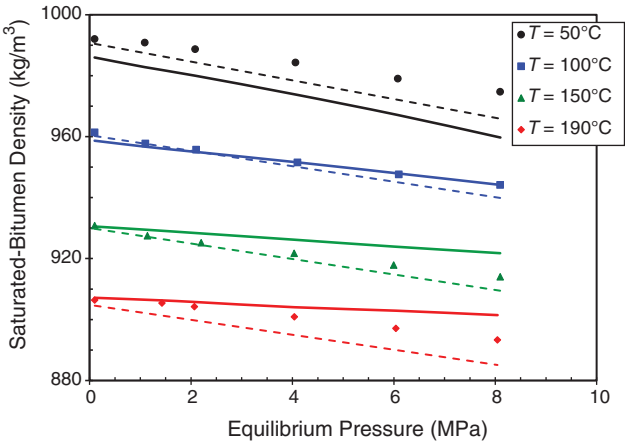

Fig. 7—Comparison of measured (symbols) and predicted saturated-liquid densities for methane/Athabasca-bitumen mixtures by use of lumped components as a function of equilibrium pressure at different temperatures: thick line, EOS; dashed line, effective liquid densities.

T (°C)	Exponent *n*
50	–0.686
100	–0.985
150	–1.409
190	–1.644

Table 5—Temperature-dependent binary-interaction coefficients; *T*, temperature.

derived from the extrapolated molar volume of liquid normal alkanes to obtain the effective liquid molar volumes of light normal alkanes present in the gaseous state in pure form. The authors plotted the molar volume of liquid normal alkanes with respect to the molecular weight and extrapolated the curve to determine the effective liquid molar volumes of light normal alkanes. Tharanivasan et al. (2011) reported the effective liquid densities for normal alkanes at pressures greater than 10 MPa.

Recently, Saryazdi (2012) found that the correlation proposed by Tharanivasan et al. (2011) resulted in higher values for the molar volumes of the lightest liquid *n*-alkanes. Saryazdi (2012) explained this overprediction by the proximity of the *n*-alkanes to their critical points and proposed a plot of the molar volumes of only the higher *n*-alkanes. Saryazdi (2012) found a linear molar volume trend for the higher *n*-alkanes and redeveloped the effective-density correlation by use of the molar volumes of the higher liquid *n*-alkanes, the molar volumes of which were linearly related to their molecular weight. Thus, the higher *n*-alkane molar volumes at fixed temperatures and pressures were extrapolated linearly to determine new effective molar volumes for the lighter *n*-alkanes. The effective molar volumes were then converted to density and plotted vs. pressure at fixed temperatures. Saryazdi et al. (2013) proposed the following equation for the effective densities of methane:

$$\rho = 532.157 - 0.69737T + (0.4261 + 1.1426 \times 10^{-3}T)P, \quad \ldots\ldots\ldots\ldots\ldots\ldots (20)$$

where ρ is the density in kg/m^3, T is the temperature in K, and P is pressure in MPa.

The measured densities of the methane/bitumen were predicted by use of Eq. 19 along with the effective densities of methane obtained by use of Eq. 20. The results are accurately predicted with this approach and are shown in Fig. 7. As anticipated from Fig. 7, the application of the effective liquid densities for the prediction of mixture densities resulted in close agreement between the measured and calculated data. **Table 6** summarizes the calculated deviations of the models for predicting the mixture densities. As the deviations show, the effective-liquid-density approach and Peng-Robinson EOS (Robinson and Peng 1978) gave almost the same predictions, whereas the effective-liquid-density approach provided lower maximum absolute deviation.

Prediction of Liquid Viscosities

The viscosity data were also correlated with the Pedersen viscosity correlation (Pedersen et al. 1984), which is modeled after the corresponding state. This model calculated the viscosity of the mixture with respect to a reference substance at the same reduced pressure and temperature. Pedersen et al. (1984) proposed the correlation,

$$\frac{\mu_{\text{mix}}(T,P)}{\mu_{\text{ref}}(T_{\text{ref}},P_{\text{ref}})} = \left(\frac{T_{c,\text{mix}}}{T_{c,\text{ref}}}\right)^{-1/6} \left(\frac{P_{c,\text{mix}}}{P_{c,\text{ref}}}\right)^{2/3} \times \left(\frac{MW_{\text{mix}}}{MW_{\text{ref}}}\right)^{1/2} \left(\frac{\beta_{\text{mix}}}{\beta_{\text{ref}}}\right), \quad \ldots\ldots\ldots\ldots (21)$$

where the molecular weight (MW) is calculated through weight averaged and molar average values as

$$MW_{\text{mix}} = d_1 (MW_w^{d_2} - MW_n^{d_2}) + MW_n. \quad \ldots\ldots\ldots\ldots (22)$$

Calculation Method	Average Absolute Relative Deviation (%)	Average Absolute Deviation (kg/m^3)	Maximum Absolute Deviation (kg/m^3)
Peng-Robinson (Robinson and Peng 1978)	0.45	4.5	15.0
Effective liquid density	0.48	4.2	8.2

Table 6—The deviations of different models for the calculation of densities of the methane/Athabasca-bitumen mixture.

The rotational coefficient proposed by Pedersen et al. (1984) to account for the deviation from the simple corresponding state is defined as

$$\beta = 1 + d_3 \left(\frac{\rho}{\rho_c}\right)^{d_4}_{\text{ref}} MW_{\text{mix}}^{d_5}. \quad \ldots\ldots\ldots\ldots\ldots\ldots (23)$$

A modified version of the Pedersen et al. (1984) correlation for methane viscosity (Pedersen and Fredenslund 1987) was used to correlate the viscosity data. The coefficients (d_i) were adjusted to match the viscosity data. The best-fitted coefficients are summarized in **Table 7,** and the calculated average absolute relative deviation by use of corresponding state was 16.3%.

Fig. 8 shows the measured and correlated viscosity data vs. pressure at different temperatures. The solid lines denote the results correlated by correlation, and the symbols show the experimental data. Fig. 8 illustrates that the viscosity of methane-saturated bitumen reduces with equilibrium pressure because of higher dissolution of methane and decreases with temperature because of the bitumen-viscosity variation with temperature. The effect of methane dissolution on the viscosity reduction is more pronounced at lower temperatures. As depicted in Fig. 8, the viscosity data are well-fitted with the Pedersen et al. (1984) correlation. Fig. 8 illustrates that the results of the viscosity model deviate from experimental values at low temperatures and high equilibrium pressures. However, as the temperature increases, the deviation of the model from experiments becomes less pronounced. Overall, the model correlates the viscosity data well over the studied pressure and temperature ranges.

Equilibrium *k*-Values for Reservoir Simulation

The experimental solubility and density data for the pseudobinary systems of solvent/bitumen could provide appropriate thermodynamic and phase-behavior models for reservoir-simulation software. An approach for the thermodynamic modeling and equilibrium calculation rather than equation-of-state (EOS) tuning is by use of the experimental *k*-values. Thus, on the basis of experiments, the equilibrium *k*-values for different components present in the mixture are obtained and directly applied into reservoir-simulation software. There are some experimental equilibrium *k*-values reported in the literature for methane/bitumen mixtures at vapor/liquid-equilibrium condition (Frauenfeld et al. 2002). These values can be directly used as input information for reservoir-simulation software, especially semicompositional simulators such as CMG-STARS. In addition, these values are usually used as matching parameters in the EOS models to tune the unknown parameters.

The phase-behavior experimental studies for solvent/bitumen are time-consuming and expensive; therefore, only limited operational conditions can be considered for these systems. The *k*-values were calculated for methane, and the *k*-values for bitumen components were considered zero because almost no component from bitumen is vaporized into the vapor phase. In this study, the *k*-values were calculated by

$$k = \frac{y_{CH_4}}{x_{CH_4}}, \quad \ldots\ldots\ldots\ldots\ldots\ldots\ldots\ldots\ldots\ldots (24)$$

d_1	d_2	d_3	d_4	d_5
0.0001565	2.4877	0.0005142	4.7359	0.3542

Table 7—The best-fitted coefficients and exponents of Pedersen et al. (1984) model.

where y_{CH_4} and x_{CH_4} are the mole fractions of methane in equilibrium-vapor and -liquid phases, respectively. The equilibrium gases for all experiments were analyzed with a Varian GC3900, and the results indicated that the vapor phase was virtually pure methane. Therefore, $y_{CH_4} = 1$ was considered for all temperatures and pressures. The values for x_{CH_4} were obtained by use of the data presented in Table 3 along with the molecular-weight measurements. The measured *k*-values for the methane/Athabasca-bitumen system are plotted as a function of pressure in **Fig. 9.** The *k*-values at temperatures of 50, 100, 150, and 190°C over the pressure range of 1–8 MPa are presented in Fig. 9.

For the methane/bitumen system, the methane composition in the vapor phase is almost constant; therefore, its value is determined by the composition of methane in the liquid phase. Higher solubility resulted in lower *k*-value. As depicted in Fig. 9, the increase in pressure or the decrease in temperature leads to lower *k*-values. The *k*-values for the methane/bitumen mixtures are in the range of 4–16 in the studied temperature and pressure ranges.

The generated experimental *k*-values provide the basic data and mechanistic understanding needed for quantitative assessments of any solvent-assisted process. To have more equilibrium *k*-value data, the developed EOS model can be extrapolated or interpolated to investigate the phase behavior for conditions where no experimental data were measured.

Conclusion

Vapor/liquid measurements for methane/bitumen indicated that the dissolution of gas solvent in bitumen leads to viscosity and density reduction proportional to the solubility of the solvent in bitumen. The solubility increased with increasing pressure and decreased when the temperature increased.

The effect of temperature on the solubility profile of the methane/bitumen system was negligible at high temperature, and there was a distinct difference in the solubility data at 50°C compared with the other isotherms (100, 150, and 190°C). Therefore, a reduction in viscosity at higher temperatures was less compared with a similar reduction at low temperature (50°C). There was a linear relationship between the methane-saturated viscosity and density, as well as pressure, for all temperatures. The solubilities and saturated-liquid densities were well-predicted with the Peng-

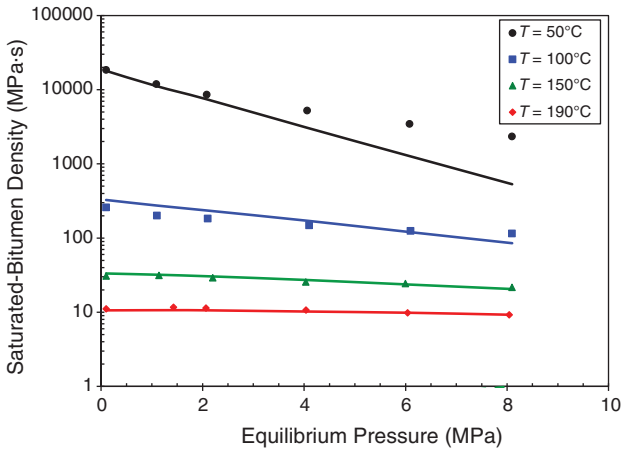

Fig. 8—Comparison of measured (symbols) and predicted saturated-liquid viscosities (lines) for methane/Athabasca bitumen mixtures by use of lumped components as a function of equilibrium pressure at different temperatures.

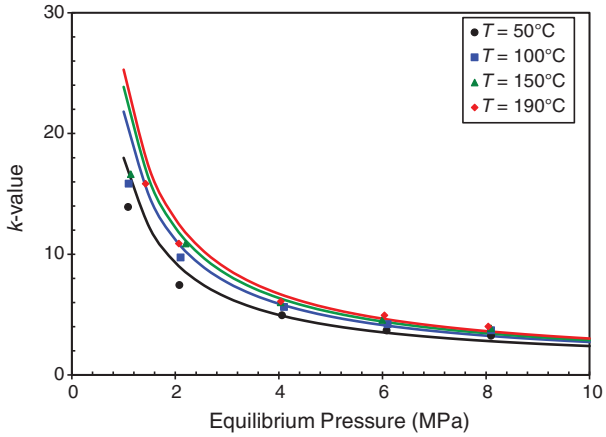

Fig. 9—Measured (symbols) vs. calculated (lines) *k*-value for methane/Athabasca-bitumen mixtures as a function of pressure at different temperatures.

Robinson equation of state (Robinson and Peng 1978) considering temperature-dependent binary-interaction parameters and volume-translation values. The saturated-liquid viscosities were adequately represented by the Pedersen et al. (1984) correlation at different temperatures and pressures.

Nomenclature

a = van der Waals attractive term
b = covolume
k = equilibrium k-value
MW = molecular weight
n = exponent in mixing rule
N_c = carbon number
P = pressure
R = gas constant
SG = specific gravity
T = temperature
T_b = boiling-point temperature
v = molar volume
w = weight fraction
x = mole fraction
y = mole fraction
Z = compressibility factor
β = rotational coefficient
δ = Peng-Robinson binary-interaction coefficient (Robinson and Peng 1978)
κ = acentric factor vapor-pressure function for Peng-Robinson equation of state (Robinson and Peng 1978)
λ = function to match vapor pressures for Peng-Robinson equation of state (Robinson and Peng 1978)
μ = dynamic viscosity
ρ = density
υ = molar volume
ω = acentric factor

Subscripts

c = critical
ref = reference
mix = mixture

Acknowledgments

The authors wish to express their appreciation for the financial support of all member companies/organizations of the SHARP consortium: Alberta Innovates Energy and Environment Solutions, Athabasca Oil Sands, Brion Energy, BP Canada, Cenovus Energy, Chevron Energy Technology, Computer Modelling Group, ConocoPhillips Canada, Devon Canada, Foundation CMG, Husky Energy, Japan Canada Oil Sands Limited, Nexen, Laricina Energy, Natural Sciences and Engineering Research Council of Canada, N-Solv Co., OSUM Oil Sands, PennWest Energy, Statoil Canada, Suncor Energy, and Total E&P Canada. The Department of Chemical and Petroleum Engineering at the University of Calgary is also acknowledged.

References

Alboudwarej, H., Akbarzadeh, K., Beck, J., et al. 2003. Regular Solution Model for Asphaltene Precipitation from Bitumens and Solvents. *AIChE J.* **49** (11): 2948–2956. http://dx.doi.org/10.1002/aic.690491124.

Al-Murayri, M. T., Harding, T. G. and Maini, B. B. 2011. Impact of Noncondensable Gas on Performance of Steam-Assisted Gravity Drainage. *J Can Pet Technol* **50** (7–8): 46–54. SPE-148943-PA. http://dx.doi.org/10.2118/148943-PA.

ASTM 2007-11, Standard Test Method for Characteristic Groups in Rubber Extender and Processing Oils and Other Petroleum-Derived Oils by the Clay-Gel Absorption Chromatographic Method. 2011. West Conshohocken, Pennsylvania, USA: ASTM International. http://dx.doi.org/10.1520/D2007-11.

ASTM D7169-11. 2011. Standard Test Method for Boiling Point Distribution of Samples with Residues Such as Crude Oils and Atmospheric and Vacuum Residues by High Temperature Gas Chromatography. West Conshohocken, Pennsylvania: ASTM International. http://dx.doi.org/10.1520/D7169-11.

Bagci A. S. and Gumrah, F. 2004. Effects of CO_2 and CH_4 Addition to Steam on Recovery of West Kozluca Heavy Oil. Presented at the SPE International Thermal Operations and Heavy Oil Symposium and Western Regional Meeting, Bakersfield, California, 16–18 March. SPE-86953-MS. http://dx.doi.org/10.2118/86953-MS.

Butler, R. M. 1985. A New Approach To The Modelling Of Steam-Assisted Gravity Drainage. *J Can Pet Technol* **24** (3): 42–51. PETSOC-85-03-01. http://dx.doi.org/10.2118/85-03-01.

Butler, R. M. 1999. The Steam and Gas Push (SAGP). *J Can Pet Technol* **38** (3): 54–61. PETSOC-99-03-05. http://dx.doi.org/10.2118/99-03-05.

Butler, R. M. and Mokrys, I. J. 1991. A New Process (VAPEX) For Recovering Heavy Oils Using Hot Water And Hydrocarbon Vapour. *J Can Pet Technol* **30** (1): 97–106. PETSOC-91-01-09. http://dx.doi.org/10.2118/91-01-09.

Butler, R. M. and Stephens, D. 1981. The Gravity Drainage of Steam-Heated Heavy Oil to Parallel Horizontal Wells. *J Can Pet Technol* **20** (2): 90–96. PETSOC-81-02-07. http://dx.doi.org/10.2118/81-02-07.

Butler, R. M. and Yee, C. T. 1986. An Experimental Study of Steam Condensation in the Presence of Noncondensable Gases in Porous Media. *AOSTRA Journal of Research* **3:** 15–23.

Butler, R. M., Jiang, Q. and Yee, C. T. 2000. Steam And Gas Push (SAGP) - 3; Recent Theoretical Developments And Laboratory Results. *J Can Pet Technol* **39** (8): 51–60. PETSOC-99-23. http://dx.doi.org/10.2118/99-23.

Diaz, O. C., Modaresghazani, J., Satyro, M. A., et al. 2011. Modeling the Phase Behavior of Heavy Oil and Solvent Mixtures. *Fluid Phase Equilibr.* **304** (1–2): 74–85. http://dx.doi.org/10.1016/j.fluid.2011.02.011.

Edmunds, N. R., Kovalsky, J. A., Gittins, S. D., et al. 1994. Review of Phase A Steam-Assisted Gravity-Drainage Test. *SPE Res Eng* **9** (2): 119–124. SPE-21529-PA. http://dx.doi.org/10.2118/21529-PA.

Frauenfeld, T. W. J., Kissel, G. and Zhou, S. 2002. PVT and Viscosity Measurements for Lloydminster-Aberfeldy and Cold Lake Blended Oil Systems. Presented at Canadian International Petroleum Conference, Calgary, Alberta, Canada, 11–13 June. PETSOC-2002-110. http://dx.doi.org/10.2118/2002-110.

Fu, C. T., Puttagunta, V. R. and Vilcsak, G. 1988. Gas Solubility Of Methane And Ethane In Cold Lake Bitumen At In Situ Conditions. *J Can Pet Technol* **27** (4): 79–85.

Gates, I. D. 2007. Oil Phase Viscosity Behavior in Expanding-Solvent Steam-Assisted Gravity Drainage. *J. Pet. Sci. Eng.* **59** (1): 123–134. http://dx.doi.org/10.1016/j.petrol.2007.03.006.

Goite, J. G., Mamora, D. D. and Ferguson, M. A. 2001. Experimental Study of Morichal Heavy Oil Recovery Using Combined Steam and Propane Injection. Presented at SPE Latin American and Caribbean Petroleum Engineering Conference, Buenos Aires, Argentina, 25–28 March. SPE-69566-MS. http://dx.doi.org/10.2118/69566-MS.

Jacobs, F. A., Donnelly, J. K., Stanislav, J., et al. 1980. Viscosity of Gas-Saturated Bitumen. *J Can Pet Technol* **19** (4): 46–50. PETSOC-80-04-03. http://dx.doi.org/10.2118/80-04-03.

Kariznovi, M., Nourozieh, H. and Abedi, J. 2010. Bitumen Characterization and Pseudocomponents Determination for EOS Modeling. *Energ. Fuel.* **24** (1): 624–633. http://dx.doi.org/10.1021/ef900886e.

Kariznovi, M., Nourozieh, H. and Abedi, J. 2011. Experimental Apparatus for Phase Behavior Study of Solvent–Bitumen Systems: A Critical Review and Design of a New Apparatus. *Fuel* **90** (2): 536–546. http://dx.doi.org/10.1016/j.fuel.2010.10.019.

Kesler, M. G. and Lee, B. I. 1976. Improve Prediction of Enthalpy of Fractions. *Hydrocarb. Process.* **55** (3): 153–158.

Kokal, S. L. and Sayegh, S. G. 1990. Gas-Saturated Bitumen Density Predictions Using The Volume-Translated Peng-Robinson Equation Of State. *J Can Pet Technol* **29** (6): 31–39. PETSOC-90-05-07. http://dx.doi.org/10.2118/90-05-07.

Lee, B. I. and Kesler, M. G. 1975. A Generalized Thermodynamic Correlation Based on Three-Parameter Corresponding States. *AIChE J.* **21** (3): 510–527. http://dx.doi.org/10.1002/aic.690210313.

Mehrotra, A. K. and Svrcek, W. Y. 1985a. Viscosity, Density and Gas Solubility Data for Oil Sand Bitumens. Part II: Peace River Bitumen Saturated with N_2, CO, CH_4, CO_2 and C_2H_6. *AOSTRA Journal of Research* **1** (4): 269–279.

Mehrotra, A. K. and Svrcek, W. Y. 1985b. Viscosity, Density and Gas Solubility Data for Oil Sand Bitumens. Part III: Wabasca Bitumen Saturated with N_2, CO, CH_4, CO_2 and C_2H_6. *AOSTRA Journal of Research* **2** (2): 83–93.

Mehrotra, A. K. and Svrcek, W. Y. 1988. Properties of Cold Lake Bitumen Saturated with Pure Gases and Gas Mixtures. *Can. J. Chem. Eng.* **66** (4): 656–665. http://dx.doi.org/10.1002/cjce.5450660419.

Mehrotra, A. K., Sarkar, M. and Svrcek, W. Y. 1985. Bitumen Density and Gas Solubility Predictions Using the Peng Robinson EOS. *AOSTRA Journal of Research* **1** (4): 215–229.

Nourozieh, H., Kariznovi, M. and Abedi, J. 2012. Development and Evaluation of a Modified Experimental Apparatus for Phase Behavior Study of Solvent–Heavy Crude Systems. *Fuel Processing Technol.* **102** (October): 116–123. http://dx.doi.org/10.1016/j.fuproc.2012.04.032.

Nourozieh, H., Kariznovi, M. and Abedi, J. 2015. Experimental and Modeling Studies of Phase Behavior for Propane/Athabasca Bitumen Mixtures. *Fluid Phase Equilib.* **397:** 37–43. http://dx.doi.org/10.1016/j.fluid.2015.03.047.

Oellrich, L., Plöcker, U., Prausnitz, J. M., et al. 1981. Equation-of-State Methods for Computing Phase Equilibria and Enthalpies. *International Chemical Engineering* **21** (1): 1–15.

Pedersen, K. S. and Fredenslund, Aa. 1987. An Improved Corresponding States Model for the Prediction of Oil and Gas Viscosities and Thermal Conductivities. *Chem. Eng. Sci.* **42** (1): 182–186. http://dx.doi.org/10.1016/0009-2509(87)80225-7.

Pedersen, K. S., Fredenslund, Aa., Christensen, P. L., et al. 1984. Viscosity of Crude Oils. *Chem. Eng. Sci.* **39** (6): 1011–1016. http://dx.doi.org/10.1016/0009-2509(84)87009-8.

Pedersen, K. S., Milter, J. and Sørensen, H. 2004. Cubic Equations of State Applied to HT/HP and Highly Aromatic Fluids. *SPE J.* **9** (2): 186–192. SPE-88364-PA. http://dx.doi.org/10.2118/88364-PA.

Peneloux, A., Rauzy, E. and Freze, R. 1982. A Consistent Correction for Redlich-Kwong-Soave Volumes. *Fluid Phase Equilibr.* **8** (1): 7–23. http://dx.doi.org/10.1016/0378-3812(82)80002-2.

Riazi, M. R. 2005. *Characterization and Properties of Petroleum Fractions*, first edition. West Conshohocken, Pennsylvania: ASTM International.

Robinson, D. B. and Peng, D. Y. 1978. The Characterization of the Heptanes and Heavier Fractions for the GPA Peng-Robinson Programs. Research Report RR-28, Gas Processors Association, Tulsa, Oklahoma.

Saryazdi, F. 2012. *Density Prediction for Mixtures of Heavy Oil and Solvents*. Master's thesis, University of Calgary, Calgary, Alberta, Canada (August 2012).

Saryazdi, F., Motahhari, H., Schoeggl, F., et al. 2013. Density of Hydrocarbon Mixtures and Bitumen Diluted with Solvents and Dissolved Gases. *Energ. Fuel.* **27** (7): 3666–3678. http://dx.doi.org/10.1021/ef400330j.

Svrcek, W. Y. and Mehrotra, A. K. 1982. Gas Solubility, Viscosity and Density Measurements for Athabasca Bitumen. *J Can Pet Technol* **21** (4): 31–38. PETSOC-82-04-02. http://dx.doi.org/10.2118/82-04-02.

Svrcek, W. Y. and Mehrotra, A. K. 1989. Properties of Peace River Bitumen Saturated with Field Gas Mixtures. *J Can Pet Technol* **28** (2): 50–56. PETSOC-89-02-01. http://dx.doi.org/10.2118/89-02-01.

Tharanivasan, A., Yarranton, H. and Taylor, S. 2011. Application of a Regular Solution-Based Model to Asphaltene Precipitation from Live Oils. *Energ. Fuel.* **25** (2): 528–538. http://dx.doi.org/10.1021/ef101076z.

Twu, C. H. 1984. An Internally Consistent Correlation for Predicting the Critical Properties and Molecular Weights of Petroleum and Coal-Tar Liquids. *Fluid Phase Equilibr.* **16** (2): 137–150. http://dx.doi.org/10.1016/0378-3812(84)85027-X.

Whitson, C. 1983. Characterizing Hydrocarbon Plus Fractions. *SPE J.* **23** (4): 683–694. SPE-12233-PA. http://dx.doi.org/10.2118/12233-PA.

Zirrahi, M., Hassanzadeh, H., Abedi, J., et al. 2014. Prediction of Solubility of CH_4, C_2H_6, CO_2, N_2 and CO in Bitumen. *Can. J. Chem. Eng.* **92** (3): 563–572. http://dx.doi.org/10.1002/cjce.21877.

Hossein Nourozieh is currently a reservoir-simulation engineer at the Computer Modelling Group (CMG) in the areas of phase-behavior study and thermal and hybrid (solvent, steam, steam/solvent) in-situ recovery processes. He has extensive experience in developing phase-behavior models, conducting reservoir simulation of heavy-oil- and bitumen-recovery processes as well as solvent-based recovery processes, designing and fabricating phase-behavior experimental systems, acquiring data for bitumen/solvent mixtures, and optimizing operational conditions for supercritical fluid extraction of oil sands. Nourozieh has also conducted research on the simulation study of underground-coal gasification, streamline simulation, and asphaltene precipitation and deposition. Before joining CMG, Nourozieh worked as a research engineer for the SHARP Consortium at the University of Calgary. He has authored or coauthored 50 journal publications and annual industry-progress reports. Nourozieh is a member of SPE and the Association of Professional Engineers and Geoscientists of Alberta. He holds a bachelor's degree in reservoir engineering from Petroleum University of Technology, Iran; a double master's degree in petroleum engineering from the University of Calgary and Petroleum University of Technology, Iran; and a PhD degree in petroleum engineering from the University of Calgary.

Mohammad Kariznovi is currently a thermal reservoir engineer at Husky Energy, working on thermal recovery of heavy oil and bitumen. He has worked on reservoir simulation, wellbore modeling and optimization, technologies development, and optimization of oil-sands recovery from the Clearwater and Grand Rapid formations. Kariznovi also performed production monitoring and well surveillance for production optimization. His research interests include asphaltene precipitation and deposition in porous media, underground-coal gasification, and streamline simulation, and he has extensive experience on phase-behavior experimental and modeling study of bitumen/solvent systems. Before joining Husky, Kariznovi worked as a researcher for the SHARP Consortium at the University of Calgary. He has authored or coauthored 50 journal publications and annual industry-progress reports. Kariznovi is a member of SPE and the Association of Professional Engineers and Geoscientists of Alberta. He holds a bachelor's degree in reservoir engineering from Petroleum University of Technology, Iran; a master's degree in reservoir engineering from the University of Calgary/Petroleum University of Technology (dual-degree collaboration program); and a PhD degree from the University of Calgary in petroleum engineering.

Jalal Abedi is a professor of chemical and petroleum engineering at the University of Calgary. He leads a phase equilibrium research facility and a research group of 20 people that is involved in research related to experimental measurements of heavy-oil/solvent/steam-phase equilibrium and equation-of-state modeling and simulation of transport processes. Abedi holds the Natural Sciences and Engineering Research Council of Canada Industrial Research Chair in Solvent Enhanced Recovery Processes. He has authored or coauthored more than 120 peer-reviewed-journal papers. Abedi is a member of SPE and the Association of Professional Engineers and Geoscientists of Alberta. He earned a bachelor's degree in chemical/petroleum engineering from Abadan Institute of Technology, Iran, and master's and PhD degrees in chemical engineering from the University of Toronto.